Parton densities from LHC vector boson production at small and large transverse momenta

Michael Klasen* and Matthias Brandt†

Institut für Theoretische Physik, Westfälische Wilhelms-Universität Münster, Wilhelm-Klemm-Straße 9, D-48149 Münster, Germany

(Received 2 July 2013; published 3 September 2013)

The parton densities of the proton are of fundamental importance not only for our description of hadronic and nuclear structure, but also for reliable predictions for new heavy-particle searches at colliders. At the large partonic momentum fractions required for the production of these particles, the parton distribution functions—in particular, that of the gluon—are unfortunately still badly constrained. In this paper, we investigate the possibility to improve on their determination with new data coming from electroweak vector boson production at large transverse momenta at the LHC with center-of-mass energies of 7, 8, or 14 TeV. We demonstrate that this process is dominated by quark-gluon scattering, that theoretical predictions can be reliably made on the basis of next-to-leading order perturbation theory and its resummation, and that these data should thus be used in global fits. We also point out that the nonperturbative parameters determined from Tevatron Run 1 Z-boson data at low p_T describe very well the new LHC data at $\sqrt{s} = 7$ TeV.

DOI: 10.1103/PhysRevD.88.054002 PACS numbers: 12.38.Bx, 13.85.Qk

I. INTRODUCTION

The parton distribution functions (PDFs) of the proton are of fundamental importance for modern particle physics. Not only do they describe our current knowledge about the internal structure and symmetries of this basic building block of matter and represent an important baseline for nuclear structure and deconfinement studies; they also enter into the theoretical description of all hadron collider experiments, precision determinations of Standard Model parameters, and new physics searches, in particular those at the energy frontier of the Large Hadron Collider (LHC), as only partonic, but not hadronic cross sections are calculable in perturbative QCD.

Consequently, a large part of the HERA physics program at DESY [1] and many global analysis efforts [2–5] have been devoted to improving on this knowledge over the last few decades. Deep inelastic scattering (DIS), now including a combination of H1 and ZEUS data from the HERA-1 run [1] and complemented at large values of Bjorken x by older fixed target data [6–11], still provides the most important single source of information. It constrains in particular the (valence) quark densities, as the gluon density enters only at next-to-leading order (NLO) and can thus only be determined from scaling violations. The decomposition of the light quark flavors can then be constrained by neutrino structure function data [12,13], and the strange quark density derived from dimuon production in neutrino DIS [14,15], while the charm structure function F_2^c, and to a lesser extent F_2^b for the bottom quark, are directly accessible at HERA [16–22].

Traditionally, the gluon density has long been constrained with prompt photon data [23] through the QCD Compton process $qg \to q\gamma$. However, photon isolation and fragmentation uncertainties have proven difficult to overcome (the situation is only now improving with the advent of the LHC data [24]), and long-standing disagreements in the low-transverse-momentum (p_T) regime have given rise to speculations on the importance of an intrinsic p_T of the partons in the proton [25]. Recent global analyses [2–5] therefore abstain from the use of prompt photon data, replacing it with better understood data (e.g. due to new jet algorithms) on inclusive jet production from DIS at HERA [26–28] (but so far, not from photoproduction [29–31], due to the uncertainty on the photon structure function [32]) and from proton-antiproton collisions at the Tevatron [33–37]. On the other hand, the Drell-Yan-like production of electroweak W [38–41] and Z [42] bosons through quark-antiquark fusion to charged leptons and neutrinos helps to constrain the up and down quark and antiquark densities with a different weighting than DIS data [43].

In two previous publications that have received considerable attention [45,46], E. L. Berger and one of us (M. K.) pointed out the possibility to use lepton pairs with relatively small invariant mass M as a surrogate for prompt photons. We demonstrated that at intermediate values of p_T of the lepton pair, its production begins to be dominated by a QCD "Compton" process $qg \to q\gamma^*$, with the real photon replaced by a virtual photon that transforms subsequently into a low-mass lepton pair. This would allow us to use this process for the determination of the gluon density also in fixed-target experiments and at large x, where it is badly constrained, while M and p_T are still high enough to allow for the application of perturbative QCD. This was established by comparing a calculation with soft-gluon resummation at the next-to-leading logarithmic (NLL) level to the pure NLO result [47]. In a follow-up publication [48], we extended this idea to polarized scattering processes, pointing out the great sensitivity,

*michael.klasen@uni-muenster.de
†matthiasbrandt@uni-muenster.de

e.g. of experiments at RHIC, to the largely unconstrained polarized gluon density.

With the much higher center-of-mass energies of $\sqrt{s} = 7$ and 8 TeV that have become available at the LHC during the last three years, and that will rise to 14 TeV after the current shutdown, it is quite natural to ask if electroweak boson production cannot play a similar role to virtual photons. The reason is that at such high energies, the W- and Z-boson masses of about 80 and 91 GeV will become more and more negligible, so that quark-gluon scattering should again quickly take over from quark-antiquark scattering. Therefore, contrary to current practice, where W- and Z-boson production are only used in the Drell-Yan mode at low p_T to constrain the quark flavor decomposition, and in particular the shape of the ratio d/u (down- over up-quark PDFs) [3], it should soon become possible to better constrain the gluon density as well, in particular at large x.

This is the goal of our present work. In Sec. II, we will first review the current status of parton densities in the proton on the basis of the uncertainty estimates provided by the three widely used global analyses CT10 [2], MSTW08 [4], and NNPDF2.1 [5]. We will do this at two different scales, i.e. at the scale of the electroweak boson and at a high scale corresponding to large transverse momenta and emphasizing both the low-x and high-x regimes. In Sec. III, we will establish the reliability of our calculation by confronting it with $\sqrt{s} = 7$ TeV LHC data on Z and W production with transverse momenta up to 600 and 300 GeV, published recently by the CMS [49] and ATLAS [50] collaborations, respectively. We will in particular address the question of up to what transverse momentum soft-gluon radiation must be resummed and at which p_T the NLO perturbative calculation starts to be reliable. Section IV is devoted to an investigation of the different partonic contributions, i.e. at which p_T the quark-gluon process starts to take over from the Drell-Yan-like quark-antiquark process, while in Sec. V we make concrete predictions in the perturbative regime for W and Z production up to large transverse momenta, where the PDFs and in particular the gluon density can be constrained. For completeness, we also show the sensitivity in the low-p_T regime. Our conclusions and an outlook are given in Sec. VI.

II. CURRENT STATUS OF PARTON DENSITY UNCERTAINTIES

In this section, we briefly review the current status of parton density uncertainties in the low- and high-x regimes and their evolution from small to large scales. As a baseline, we use the best CT10 NLO global fit f_0 [2], which we show together with its uncertainty band computed as

$$\delta^+ f = \sqrt{\sum_{i=1}^{26} [\max(f_i^{(+)} - f_0, f_i^{(-)} - f_0, 0)]^2}, \quad (1)$$

$$\delta^- f = \sqrt{\sum_{i=1}^{26} [\max(f_0 - f_i^{(+)}, f_0 - f_i^{(-)}, 0)]^2}, \quad (2)$$

where $f_i^{\pm}$ are the PDFs for positive and negative variations of the PDF parameters along the ith eigenvector direction in the 26-dimensional PDF parameter space. In order to estimate the bias coming, e.g., from different parameterizations of the x dependence at the starting scale, we also show the best fits of the MSTW08 [4] and NNPDF2.1 [5] global analyses. As is usually done, we plot in all cases x times the PDF—i.e., the momentum distribution of the partons in the proton.

First, we show in Fig. 1 the gluon PDF (reduced by a factor of 20) and the up-quark and strange-quark PDFs at the factorization scale $Q = M_Z$ (top), adequate for electroweak boson production at low transverse momenta, and at the higher scale of $Q = 1$ TeV (bottom), relevant for high-p_T vector boson production. In this figure, a

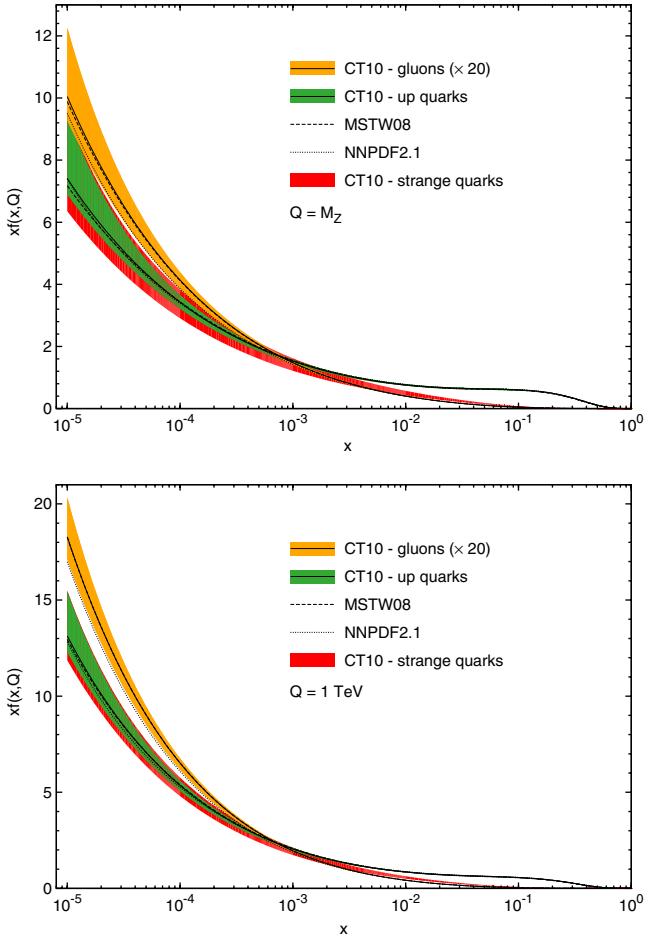

FIG. 1 (color online). Parton distribution functions (PDFs) on a logarithmic x scale, emphasizing the low-x region, at the factorization scale $Q = M_Z$ (top) and 1 TeV (bottom) from different collaborations. PDF uncertainties are only shown for the CT10 group. PDFs are printed for gluons, up quarks, and strange quarks.

logarithmic x axis has been chosen, which emphasizes the low-x regime. In this region, the sea-quark-dominated up- and strange-quark PDFs largely overlap, so only the uncertainty band is shown for the latter; the central values are omitted for better visibility. As is well known, the uncertainty highly increases below values of $x = 10^{-3}$, where little information is available from pre-LHC experiments. The evolution from low (top) to high (bottom) scales resums multiple parton splitting, increasing the densities of gluons and sea quarks at small x and at the same time reducing the (mostly valence-quark) PDFs at large x. Since the Q^2 dependence is perturbatively calculable, the PDFs at high Q become less dependent on the nonperturbative input at the starting scale Q_0, so that their uncertainty due to the fit of the unknown x dependence at Q_o to experimental data is reduced.

The shift of the up-quark PDFs, and also the gluon (and induced strange-quark) PDFs, from larger to smaller x values with the evolution from $Q = M_Z$ to $Q = 1$ TeV is more clearly visible in Fig. 2, with its linear x axis. Here, up quarks (which have a valence-quark contribution) and strange quarks (which do not) are well separated, so that we may now also show the central values for the latter. It is obvious that the CT10 uncertainty band, induced by the experimental data, does not cover in all cases the central values of MSTW08 and NNPDF2.1, demonstrating the important influence of the theoretical bias on the x parametrization at the starting scale Q_0.

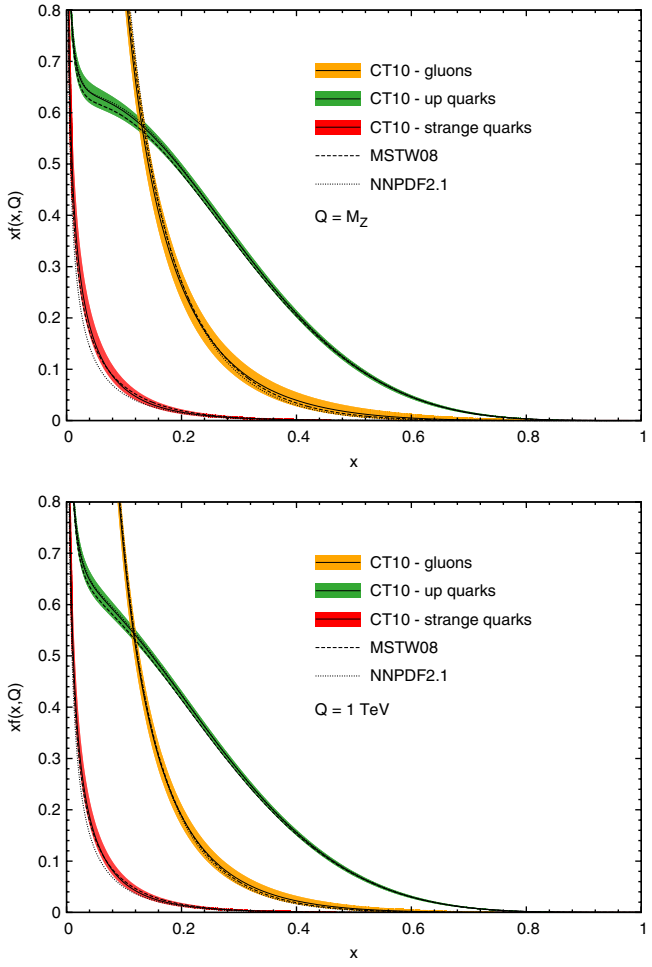

FIG. 2 (color online). Same as in Fig. 1, but on a linear x scale, emphasizing the high-x region.

If we focus now on the gluon PDF at large x, we can see that it is much less constrained than the up-quark PDF, which was directly probed at HERA and in other DIS experiments. At the lower scale $Q = M_Z$, the gluon uncertainty parametrized by CT10 at $x = 0.3$ and $x = 0.4$ is considerable: $+21\%/-18\%$ and $+40\%/-30\%$, respectively. The evolution to $Q = 1$ TeV does not significantly change this uncertainty, which there amounts to $+22\%/-17\%$ and $+43\%/-28\%$, respectively. Contrary to the strange-quark PDFs, the central MSTW08 and NNPDF2.1 gluon PDF fits are covered by the CT10 uncertainty bands.

In the three global analyses discussed above, LHC data have not yet been included. However, the new CT10 next-to-next-to-leading-order PDFs [3] have been compared with the total W and Z cross sections at 7 and 8 TeV, with the result that they agree within the still substantial errors. Also, the W and Z rapidity distributions, as well as the W charge asymmetry, at 7 TeV have been found to agree within errors. These data are obtained in a Drell-Yan situation at small p_T and, when included in future global PDF analyses, will mostly influence the quark PDFs at small x—in particular, the valence quarks, which are badly constrained in this region. This requires, however, that the theoretical predictions for the partonic scattering cross sections, including soft-gluon resummation, be under control [3].

III. NLO CROSS SECTIONS WITH RESUMMATION FOR THE LHC

As with our previous calculations for low-mass lepton pair production in hadron collisions [45,46], our theoretical predictions for massive electroweak gauge-boson production at the LHC are based on a full NLO calculation matched to soft-gluon resummation at the NLL level [47]. This allows us to establish in this section the regions in p_T where the perturbative results are reliable and where they have to be supplemented by a resummation procedure to all orders in the strong coupling constant α_s. This p_T resummation is based on the Collins-Soper-Sterman formalism [51] and is evaluated in impact parameter (b) space. The differential cross section for the production of a vector boson V from two hadrons h_1 and h_2 is thus written as

$$\frac{d\sigma(h_1h_2 \to VX)}{dQ^2 dp_T^2 dy} = \frac{1}{(2\pi)^2}\delta(Q^2 - M_V^2) \times \int d^2b e^{i\vec{p}_T\vec{b}}\tilde{W}_{j\bar{k}}(b, Q, x_1, x_2) + Y(p_T, Q, x_1, x_2), \quad (3)$$

where Q and y are the invariant mass and rapidity of the vector boson, respectively, and $x_{1,2} = e^{\pm y} Q/\sqrt{s}$ are the momentum fractions of the interacting partons j and $\bar{k}$. The regular piece, denoted $Y(p_T, Q, x_1, x_2)$, is obtained by subtracting the terms which are singular in p_T from the exact fixed-order result. The form factor $\tilde{W}_{j\bar{k}}(b, Q, x_1, x_2)$ can be factorized into a perturbative piece $\tilde{W}^{\rm pert}_{j\bar{k}}(b_*)$ and a nonperturbative function $\tilde{W}^{\rm NP}_{j\bar{k}}(b)$

$$\tilde{W}_{j\bar{k}}(b, Q, x_1, x_2) = \tilde{W}^{\rm pert}_{j\bar{k}}(b_*, Q, x_1, x_2)\tilde{W}^{\rm NP}_{j\bar{k}}(b, Q, x_1, x_2) \tag{4}$$

by introducing a variable

$$b_* = \frac{b}{\sqrt{1 + (b/b_{\rm max})^2}}, \tag{5}$$

which, together with $b_{\rm max} = 0.5\ {\rm GeV}^{-1}$, ensures the perturbativity of $\tilde{W}^{\rm pert}_{j\bar{k}}$. A renormalization group analysis [51] exhibits a logarithmic dependence of the nonperturbative function $\tilde{W}^{\rm NP}_{j\bar{k}}(b, Q, Q_0, x_1, x_2)$ on the starting scale Q_0 of the PDFs, which, however, turns out to be negligible in practice. Its b and x dependences must be fitted to experimental data. We use a Gaussian parametrization by Brock, Landry, Nadolsky, and Yuan (BLNY):

$$\tilde{W}^{\rm NP}_{j\bar{k}}(b, Q, Q_0, x_1, x_2) = \exp\left[-g_1 - g_2 \ln\left(\frac{Q}{2Q_0}\right) - g_1 g_3 \ln(100 x_1 x_2)\right] b^2, \tag{6}$$

with the three parameters $g_1 = 0.21$, $g_2 = 0.68$, and $g_3 = -0.60$ and evolved from the starting scale $Q_0 = 1.6$ GeV, which has been shown to fit the Tevatron Run 1 data on Z-boson production very well [52].

Our theoretical predictions computed in this way are compared in the upper part of Fig. 3 to CMS data on Z-boson production at $\sqrt{s} = 7$ TeV [49]. The data were presented by the CMS Collaboration normalized to the total cross section and with combined statistical and systematic uncertainties, individually for decay electrons and muons with $|\eta| < 2.1$, and as a combination. They extend to p_T values of 600 GeV for the Z boson. We only show the combination in Fig. 3, where we have multiplied our Z-boson cross section, computed with our baseline PDF set CT10 [2] and integrated over $|y| < 2.1$, with the relevant branching fractions [53]. As one can observe, the region where resummation is needed to describe the data extends to values of $p_T \simeq 75$ GeV. Below this point, the perturbative calculation (dotted) diverges logarithmically due to multiple-soft-gluon radiation and must be resummed (dashed), while above this point, the regular, nonlogarithmic terms due to hard, noncollinear radiation can no longer be neglected as is done in the resummation calculation. The failure of the soft-gluon approximation in the transition region is exhibited by the fact that the resummation prediction becomes negative there and must be matched to the perturbative result by reexpanding it, subtracting from it the divergent terms, and then adding the perturbative result to obtain a prediction valid in all regions (full curve). The comparison of our theoretical predictions with the experimental data is excellent over the full region in p_T. Similarly good agreement has been found by the CMS Collaboration with predictions based on the POWHEG NLO Monte Carlo generator with parton showers, which effectively also resum the leading logarithms at small values of p_T [54,55].

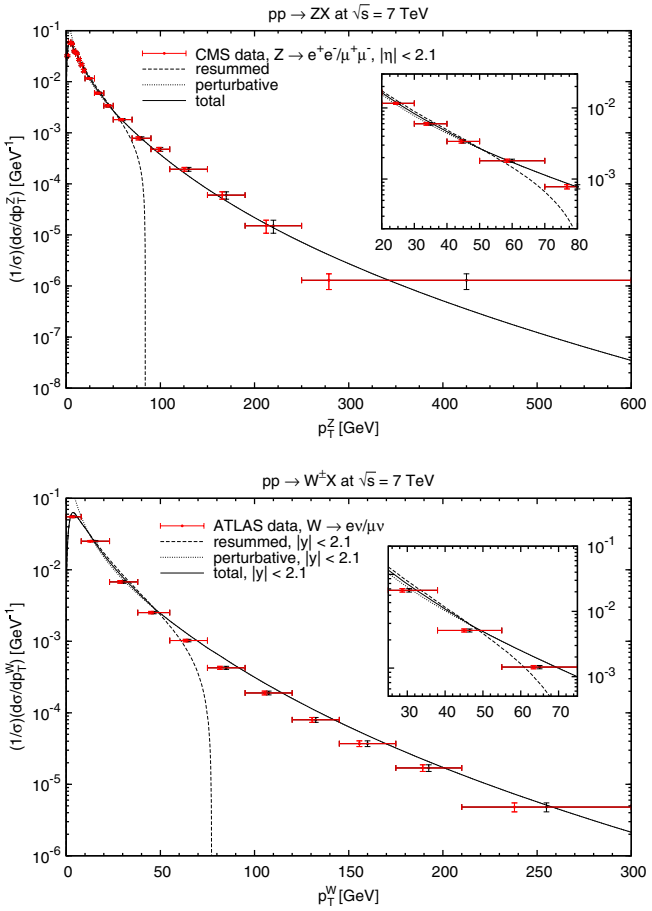

FIG. 3 (color online). Transverse-momentum spectra of Z (top) and W (bottom) bosons at the LHC with $\sqrt{s} = 7$ TeV, normalized to the total cross section. CMS (top) and ATLAS (bottom) data are compared with our theoretical calculation at NLL + NLO in the rapidity range $|y| < 2.1$ using CT10 PDFs. The data points are positioned at the theoretical centers of gravity of the bins (red) and at the centers of the bins (black).

In the lower part of Fig. 3, we compare our theoretical predictions to ATLAS data on W-boson production at $\sqrt{s} = 7$ TeV [50]. Similarly to CMS, the ATLAS Collaboration present their results normalized to the total cross section and for a combination of weak bosons decaying to electrons and muons, measured now with $|\eta| < 2.4$. The decay neutrinos of course escape detection. The p_T spectrum of the W boson is then obtained through a

two-step unfolding procedure up to values of 300 GeV. The theoretical behavior is very similar to the one for Z-boson production, except that the transition from the region dominated by large logarithms to the perturbative regime occurs at slightly smaller values of $p_T \simeq 65$ GeV. This can be attributed to the other hard scale in the process, the mass of the W boson, which is, with 80.385 GeV, somewhat smaller than the Z-boson mass of 91.188 GeV [53]. If we assume the rapidity region of the W boson, not given explicitly by the ATLAS experiment, to be $|y| < 2.1$, we obtain again very good agreement with the experimental data, although the normalization to the total cross section renders the prediction almost insensitive to the exact value of this cut. The experimentalists obtain similarly good agreement when comparing to the resummation program ResBos [52,56,57].

An important question is how the resummation and perturbative regions change when moving from current LHC experiments with $\sqrt{s} = 7$ TeV to those in the future, which will be conducted with collision energies up to 14 TeV. We have investigated this question with the result (not shown explicitly) that for Z bosons the pure resummation result then starts to deviate strongly from the total prediction at values of $p_T \simeq 90$ GeV, whereas for W bosons this point is reached at $p_T \simeq 80$ GeV. On the other hand, our calculations indicate that the reach in p_T, which was 600 (300) GeV for Z (W) bosons produced at $\sqrt{s} = 7$ TeV with an integrated luminosity of 35.9(31) pb^{-1}, should increase to the multi-TeV range—i.e., at least 2 TeV, at $\sqrt{s} = 14$ TeV and an integrated luminosity of 100 fb^{-1}. At the end of 2012 already, more than 23 fb^{-1} had been recorded by ATLAS and CMS each with $\sqrt{s} = 8$ TeV. It would thus already be interesting to analyze these data for electroweak vector boson production with high p_T.

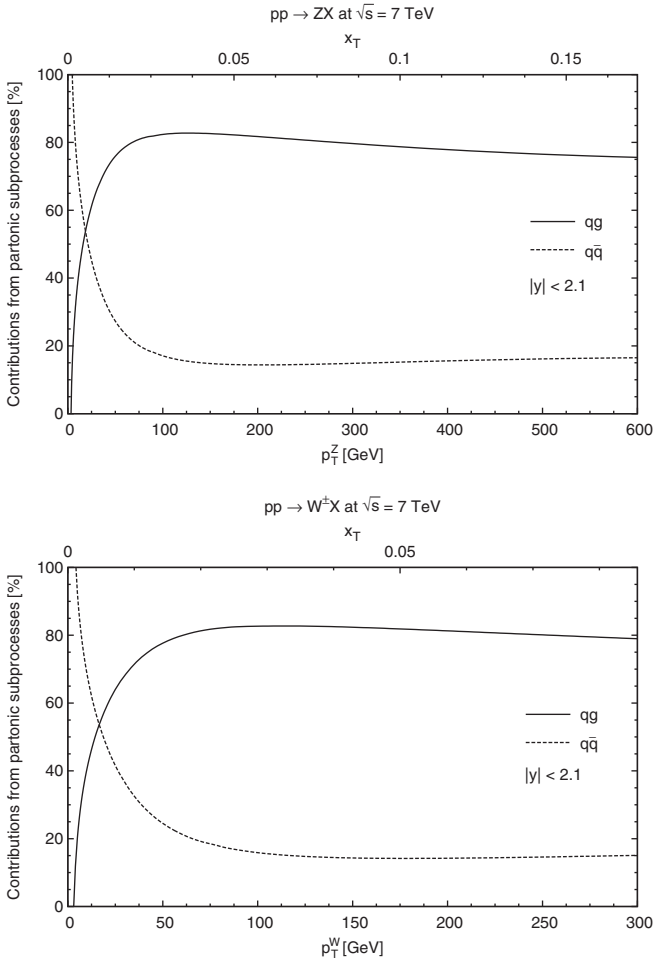

FIG. 4. Relative contributions at NLO of the quark-antiquark (dashed lines) and QCD Compton (solid lines) subprocesses to the production of Z (top) and W bosons (bottom) at the LHC with $\sqrt{s} = 7$ TeV. Subdominant partonic subprocesses which enter only at NLO or higher orders are not shown.

IV. DECOMPOSITION OF PARTONIC PROCESSES

The next question that arises is then at which values of p_T electroweak boson production starts to be dominated by the QCD Compton processes $qg \to Zq$ and $qg \to Wq$, just as low-mass lepton pairs (with invariant mass below M_W) were dominated by virtual photon radiation through the process $qg \to \gamma^* q$.

The importance of the quark-gluon scattering process is clearly visible in Fig. 4. In fact, at a proton-proton collision energy of $\sqrt{s} = 7$ TeV, it is sufficient for the transverse momentum of the produced Z (top) or W (bottom) boson to exceed 20 or 15 GeV. The quark-gluon process then remains at a level of 75%–80%, almost up to the kinematic limit—more precisely, up to 3 TeV—before quark-antiquark fusion takes over again. Note that in this figure we show only the subprocesses that exist already at leading order. At NLO and beyond, other processes like $gg \to Vq\bar{q}$ and $qq \to Vqq$ with $V = Z$, W enter as well, but they remain at the level of a few percent. This statement depends, of course, on the factorization scheme and scale, which we choose to be the $\overline{\text{MS}}$ scheme and $\mu_F = \sqrt{M_V^2 + p_T^2}$, identical to the renormalization scale μ_R. This choice should in principle provide for an optimal stability of the perturbative calculation in the low- and high-p_T regions.

The dominance of the qg subprocess persists at higher collision energies of $\sqrt{s} = 14$ TeV, as can be seen from Fig. 5. The peak contribution is even a bit larger and reaches more than 85% at $p_T \simeq 100$ GeV. A local minimum of about 70% exists at intermediate values of $p_T \simeq 1.5$ TeV. In Figs. 4 and 5 we have in addition introduced a second, upper x axis. It shows an estimator for the values of Bjorken x, more precisely $x_T = 2p_T/\sqrt{s}$, at which the parton distributions in the colliding protons are probed. It is clear that at the very large values of p_T accessible with high LHC luminosities and energies of 14 (and also 8) TeV, it should be possible to probe and constrain the gluon density where it is not well known.

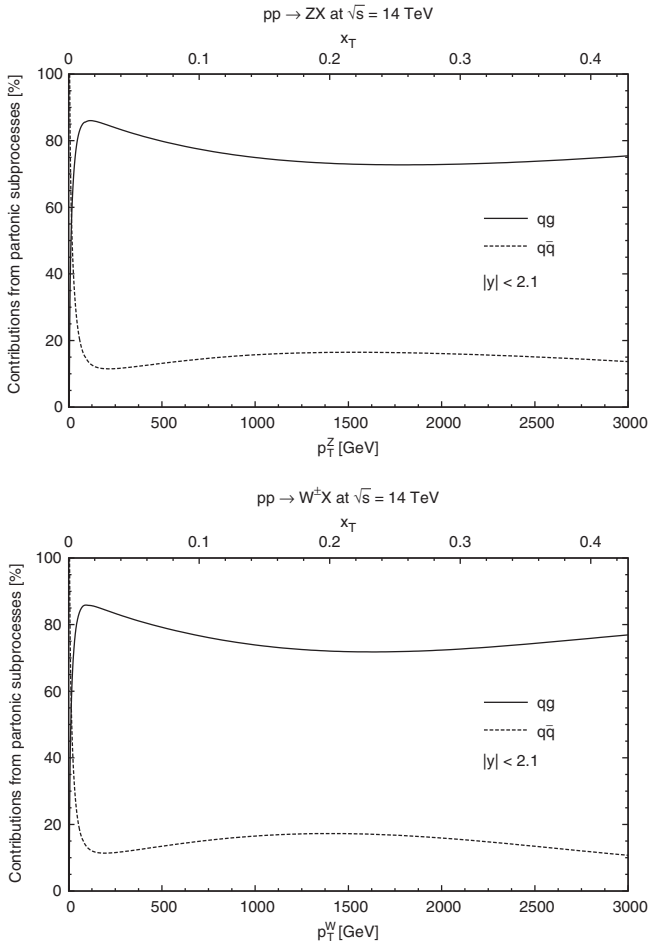

FIG. 5. Same as Fig. 4 for $\sqrt{s} = 14$ TeV.

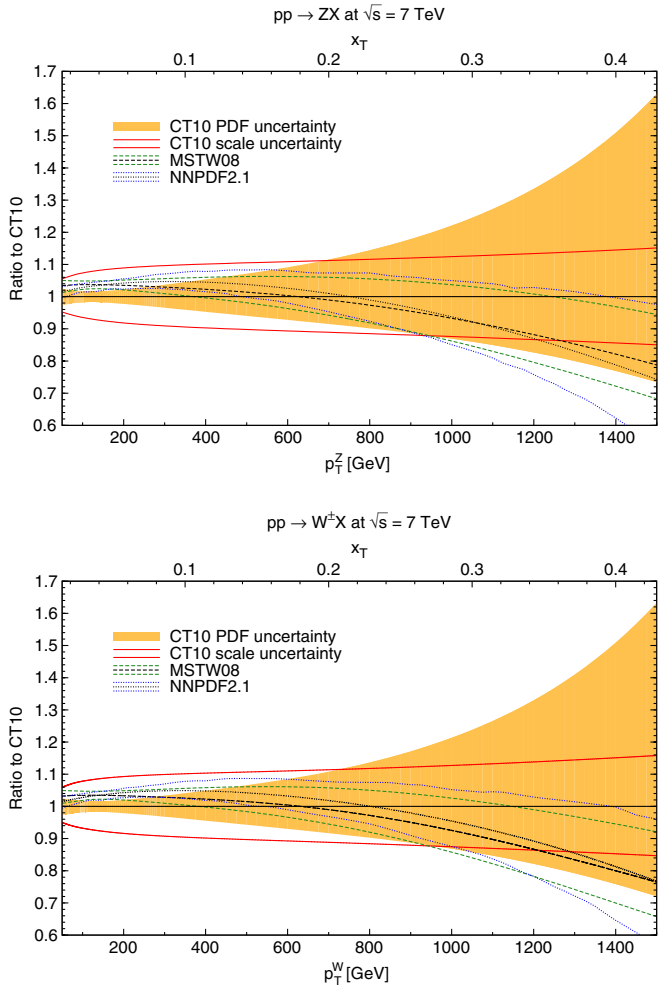

FIG. 6 (color online). Ratios of Z- (top) and W-boson (bottom) p_T distributions at $\sqrt{s} = 7$ TeV computed with different scales and PDFs to the baseline predictions with CT10 and central scale.

V. PARTON DENSITY SENSITIVITY OF LHC VECTOR BOSON PRODUCTION

Having established the reliability of our calculations in the resummation and perturbative regimes, as well as the dominance of the quark-antiquark and quark-gluon subprocesses at small and intermediate to large transverse momenta, we can now confront the current status of uncertainties on the quark and gluon PDFs in the proton with the prospects for improving on their determination with electroweak boson production at the LHC.

To this end, we compute in Fig. 6 ratios of transverse-momentum spectra for Z (top) and W (bottom) bosons using various PDFs to our baseline prediction with CT10 PDFs. While this figure shows results for the LHC with $\sqrt{s} = 7$ TeV, Fig. 7 shows these ratios for Z-boson production at a center-of-mass energy of $\sqrt{s} = 14$ TeV. If one accounts for a rescaling of transverse momenta by a factor of 2, these figures are very similar. Results for $\sqrt{s} = 8$ TeV are therefore not shown, as they lie naturally in between, close to the results of $\sqrt{s} = 7$ TeV. With a total luminosity of more than 23 fb^{-1} collected by ATLAS and CMS each at $\sqrt{s} = 8$ TeV, a range in p_T up to 1 TeV or more can be

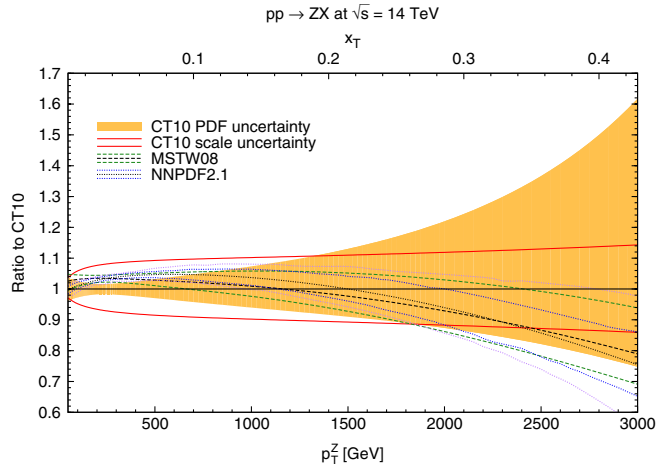

FIG. 7 (color online). Same as Fig. 6 for Z bosons at $\sqrt{s} = 14$ TeV.

expected. This corresponds to values of Bjorken x, or more precisely, x_T (upper x axis) of about 0.3 or more.

In our discussion in Sec. II, we observed that the gluon uncertainty at $x = 0.3$ and $x = 0.4$ parametrized by CT10 is quite large and reaches at the scale $Q = 1$ TeV values of $+22\%/-17\%$ and $+43\%/-28\%$, respectively. Since the QCD Compton process contributes here more than 75% to the total cross section, this uncertainty is directly reflected in Figs. 6 and 7 through the yellow CT10 uncertainty bands. The quark PDFs are dominated in this region by the valence contribution and add only a little to the total uncertainty. The alternative PDF determinations by MSTW08 (dashed) and NNPDF2.1 (dotted) follow in this region the lower boundary of the CT10 uncertainty band, which is based on a Hessian treatment of the experimental statistical error with fixed tolerance ($\Delta\chi^2 = 100$). The MSTW08 and NNPDF2.1 uncertainty bands are smaller than the one from the CT10, in particular due to a dynamic and smaller tolerance ($\Delta\chi^2 \sim 25$) and a different (Monte Carlo) sampling of the statistical error and cross-section validation, respectively, but also due to different input data, values of α_s, treatments of heavy quarks and experimental systematic errors, parametrizations, etc. The scale uncertainty (red lines), estimated in the conventional way by varying the factorization and renormalization scales simultaneously by a factor of 2 up and down about the central scale $\sqrt{M_V^2 + p_T^2}$, stays, with $\pm 10\%$ to $\pm 15\%$, considerably smaller than the CT10 PDF uncertainty alone, and of course also the envelope of all three PDF uncertainties. With threshold resummation, computed e.g. with soft collinear effective theory, the scale uncertainty reduces to about $\pm 5\%$ at large p_T [58]. Measurements of electroweak boson production with transverse momenta of 1 TeV or beyond at $\sqrt{s} = 7$, 8, or 14 TeV will thus clearly help to improve on the determination of the gluon PDF in the large-x regime.

At low p_T, corresponding to x values of 0.01 to 0.1, the situation is quite different. The quark-gluon process still dominates, but the gluon PDF is quite well determined here through the evolution with errors below 10% at the scale $Q = M_Z$ (see Sec. II). At the same time, the up- and down-quark PDFs are still strongly influenced by the well-constrained valence contribution. In contrast, the uncertainty induced by the unphysical scales persists at the level of 10% and thus represents the dominant source of theoretical uncertainty. Taken together, these observations leave little room for improvement of the gluon PDF through electroweak boson production at small transverse momenta.

Since the rapidity of the produced vector boson enters exponentially in the expressions for the partonic momentum fractions $x_{1,2}$ (see Sec. II), it is clear that moving away from central to forward rapidity creates a more asymmetric situation, where the partons of one incoming proton are probed at much larger values, and those of the other proton at much smaller values of x. This is reflected in Fig. 8,

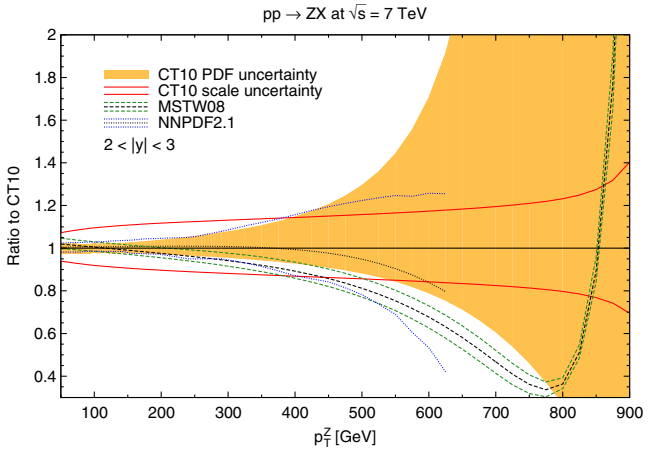

FIG. 8 (color online). Same as Fig. 6 for Z bosons at forward rapidity $|y| \in [2; 3]$.

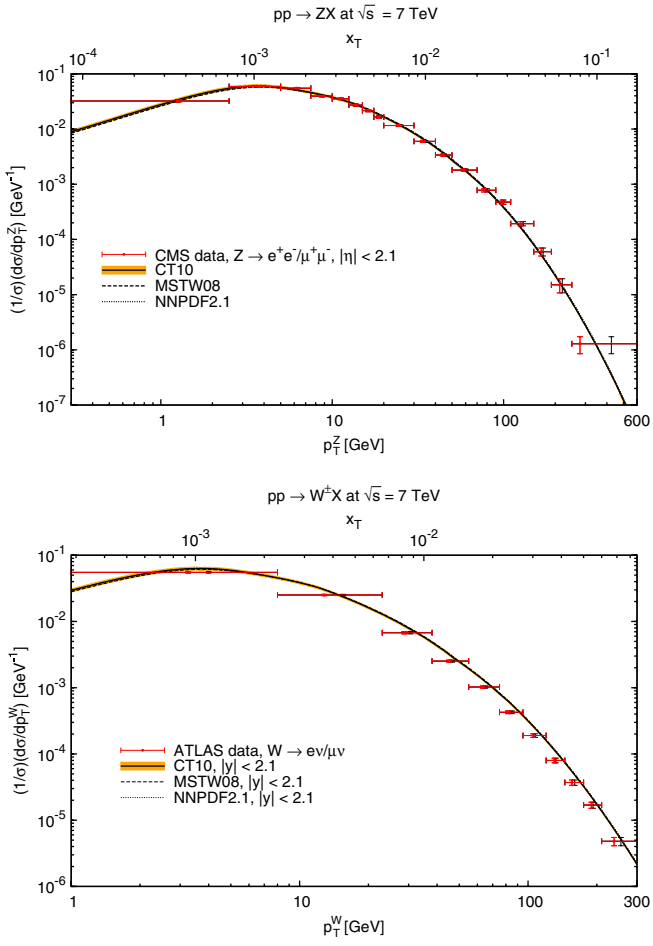

FIG. 9 (color online). Normalized transverse-momentum spectra for Z (top) and W (bottom) bosons. Our theoretical calculations at NLO combined with resummation for the rapidity range $|y| < 2.1$ and using various PDFs are shown in comparison with CMS and ATLAS data on a logarithmic x axis. The data points are positioned at the theoretical centers of gravity of the bins (red) and at the centers of the bins (black).

where we show cross-section ratios obtained with different PDFs from those obtained with CT10 for the production of electroweak bosons with rapidities of $|y| \in [2;3]$. These rapidities are still covered by the CMS and ATLAS electromagnetic endcap calorimeters, while muons are only detected up to $|\eta| < 2.4$ and 2.5, respectively. As expected, the PDF uncertainties in the forward region are much larger and reach easily a factor of 2. For the reasons mentioned above, the MSTW08 uncertainty band is much smaller than the CT10 band, but it has a very different shape, while the NNPDF2.1 band widens at the same p_T values as the CT10 band, but can even lead to negative cross sections. The envelope of all error bands is thus even larger than the error band of CT10 alone. This demonstrates the potential of corresponding measurements to pin down the gluon PDFs, depending on the transverse momenta that can be reached there.

As a final point, it is also interesting to use Fig. 9 to compare in more detail our theoretical predictions and the experimental data from CMS [49] (top) and ATLAS [50] (bottom) on Z- and W-boson production in the low-p_T regime, emphasized in this figure by the logarithmic x axis. The reason is that in this region, the theoretical prediction is also influenced by the parameters g_1, g_2, and g_3 of the nonperturbative function $\tilde{W}^{\mathrm{NP}}_{j\bar{k}}(b, Q, Q_0, x_1, x_2)$ (see Sec. III), which had been fitted only to Tevatron Run 1 data on Z-boson production, but not yet to LHC data [52]. As it can be seen from Fig. 9, this fit also allows us to describe the normalized LHC data perfectly well, so that a newer fit does not seem necessary or lead to much improvement at this point. This may, however, change once absolute cross sections become available.

VI. CONCLUSIONS

In conclusion, we have in this paper investigated a possibility to better constrain the parton densities in the proton at large momentum fractions. These parton densities are of fundamental importance not only for our description of hadronic and nuclear structure, but also for reliable predictions for new heavy-particle searches at colliders.

After establishing the current status of uncertainty from the CT10, MSTW08 and NNPDF2.1 parametrizations, we have computed perturbative and resummed cross sections for electroweak vector boson production at the LHC, finding good agreement with published CMS and ATLAS data for Z and W bosons at $\sqrt{s} = 7$ TeV up to p_T values of 600 and 300 GeV, respectively. We found that at transverse momenta beyond about 20 GeV, they were dominated by the QCD Compton process, inducing a large sensitivity of the cross sections on the gluon PDFs.

We have shown that with the luminosities reached in the 8 TeV and future 14 TeV runs, transverse momenta in the TeV range should be measurable, thus providing access to the gluon PDF at large values of x, where it is currently very badly constrained. The theoretical scale uncertainty has been shown to stay sufficiently small there.

At smaller transverse momenta, little improvement can be made on the determination of gluon and quark PDFs through the proposed process. However, the uncertainties coming from the resummation calculation—and in particular, its nonperturbative component—have been shown to be under control, as new LHC data at $\sqrt{s} = 7$ TeV can be described perfectly well with a fit made only to Tevatron Run 1 data on Z-boson production.

We therefore hope that the ATLAS and CMS collaborations will soon make available analyses of electroweak boson production at large transverse momenta, so that they can be used in future global analyses of the parton distribution functions in the proton. As we have learned, at least the NNPDF Collaboration already have concrete plans to do this [59].

ACKNOWLEDGMENTS

We thank M. Boonekamp for stimulating our interest on this topic. This work has been supported by the BMBF Theorie-Verbund "Begleitende theoretische Untersuchungen zu den Experimenten an den Großgeräten der Teilchenphysik."

[1] F. D. Aaron *et al.* (H1 and ZEUS collaborations), J. High Energy Phys. 01 (2010) 109.
[2] H.-L. Lai, M. Guzzi, J. Huston, Z. Li, P. M. Nadolsky, J. Pumplin, and C.-P. Yuan, Phys. Rev. D **82**, 074024 (2010).
[3] J. Gao, M. Guzzi, J. Huston, H.-L. Lai, Z. Li, P. Nadolsky, J. Pumplin, D. Stump *et al.*, arXiv:1302.6246.
[4] A. D. Martin, W. J. Stirling, R. S. Thorne, and G. Watt, Eur. Phys. J. C **63**, 189 (2009).
[5] R. D. Ball, V. Bertone, F. Cerutti, L. Del Debbio, S. Forte, A. Guffanti, J. I. Latorre, J. Rojo, and M. Ubiali, Nucl. Phys. **B849**, 296 (2011).
[6] A. C. Benvenuti *et al.* (BCDMS Collaboration), Phys. Lett. B **223**, 485 (1989).
[7] A. C. Benvenuti *et al.* (BCDMS Collaboration), Phys. Lett. B **237**, 592 (1990).
[8] M. Arneodo *et al.* (New Muon Collaboration), Nucl. Phys. **B483**, 3 (1997).
[9] J. P. Berge, H. Burkhardt, F. Dydak, R. Hagelberg, M. Krasny, H. J. Meyer, P. Palazzi, and F. Ranjard *et al.*, Z. Phys. C **49**, 187 (1991).
[10] U.-K. Yang *et al.* (CCFR/NuTeV Collaboration), Phys. Rev. Lett. **86**, 2742 (2001).

[11] W. G. Seligman, C. G. Arroyo, L. de Barbaro, P. de Barbaro, A. O. Bazarko, R. H. Bernstein, A. Bodek, T. Bolton *et al.*, Phys. Rev. Lett. **79**, 1213 (1997).

[12] M. Tzanov *et al.* (NuTeV Collaboration), Phys. Rev. D **74**, 012008 (2006).

[13] G. Onengut *et al.* (CHORUS Collaboration), Phys. Lett. B **632**, 65 (2006).

[14] M. Goncharov *et al.* (NuTeV Collaboration), Phys. Rev. D **64**, 112006 (2001).

[15] A. O. Bazarko *et al.* (CCFR Collaboration), Z. Phys. C **65**, 189 (1995).

[16] H1 Collaboration, Z. Phys. C **72**, 593 (1996).

[17] H1 Collaboration, Phys. Lett. B **528**, 199 (2002).

[18] H1 Collaboration, Eur. Phys. J. C **45**, 23 (2006).

[19] H1 Collaboration, Eur. Phys. J. C **40**, 349 (2005).

[20] J. Breitweg *et al.* (ZEUS Collaboration), Eur. Phys. J. C **12**, 35 (2000).

[21] S. Chekanov *et al.* (ZEUS Collaboration), Phys. Rev. D **69**, 012004 (2004).

[22] S. Chekanov *et al.* (ZEUS Collaboration), J. High Energy Phys. 07 (2007) 074.

[23] M. Bonesini *et al.* (WA70 Collaboration), Z. Phys. C **38**, 371 (1988).

[24] D. d'Enterria and J. Rojo, Nucl. Phys. **B860**, 311 (2012).

[25] L. Apanasevich *et al.* (Fermilab E706 Collaboration), Phys. Rev. Lett. **81**, 2642 (1998).

[26] S. Chekanov *et al.* (ZEUS Collaboration), Phys. Lett. B **547**, 164 (2002).

[27] S. Chekanov *et al.* (ZEUS Collaboration), Nucl. Phys. **B765**, 1 (2007).

[28] H1 Collaboration, Phys. Lett. B **653**, 134 (2007).

[29] M. Klasen, G. Kramer, and S. G. Salesch, Z. Phys. C **68**, 113 (1995).

[30] M. Klasen and G. Kramer, Z. Phys. C **72**, 107 (1996).

[31] M. Klasen and G. Kramer, Z. Phys. C **76**, 67 (1997).

[32] S. Albino, M. Klasen, and S. Soldner-Rembold, Phys. Rev. Lett. **89**, 122004 (2002).

[33] A. Abulencia *et al.* (CDF Collaboration), Phys. Rev. D **75**, 092006 (2007); **75**, 119901(E) (2007).

[34] T. Aaltonen *et al.* (CDF Collaboration), Phys. Rev. D **78**, 052006 (2008); **79**, 119902(E) (2009).

[35] V. M. Abazov *et al.* (D0 Collaboration), Phys. Rev. Lett. **101**, 062001 (2008).

[36] M. Klasen and G. Kramer, Phys. Lett. B **386**, 384 (1996).

[37] M. Klasen and G. Kramer, Phys. Rev. D **56**, 2702 (1997).

[38] D. Acosta *et al.* (CDF Collaboration), Phys. Rev. D **71**, 051104 (2005).

[39] V. M. Abazov *et al.* (D0 Collaboration), Phys. Rev. D **77**, 011106 (2008).

[40] V. M. Abazov *et al.* (D0 Collaboration), Phys. Rev. Lett. **101**, 211801 (2008).

[41] F. Abe *et al.* (CDF Collaboration), Phys. Rev. Lett. **81**, 5754 (1998).

[42] V. M. Abazov *et al.* (D0 Collaboration), Phys. Rev. D **76**, 012003 (2007).

[43] For a recent study of the sensitivity of W^+/W^- and $W^\pm/Z$ production ratios at the LHC on the up- and down-quark PDFs, see Ref. [44].

[44] S. A. Malik and G. Watt, arXiv:1304.2424.

[45] E. L. Berger, L. E. Gordon, and M. Klasen, Phys. Rev. D **58**, 074012 (1998).

[46] E. L. Berger and M. Klasen, Nucl. Phys. B, Proc. Suppl. **82**, 179 (2000).

[47] P. B. Arnold and R. P. Kauffman, Nucl. Phys. **B349**, 381 (1991).

[48] E. L. Berger, L. E. Gordon, and M. Klasen, Phys. Rev. D **62**, 014014 (2000).

[49] S. Chatrchyan *et al.* (CMS Collaboration), Phys. Rev. D **85**, 032002 (2012).

[50] G. Aad *et al.* (ATLAS Collaboration), Phys. Rev. D **85**, 012005 (2012).

[51] J. C. Collins, D. E. Soper, and G. F. Sterman, Nucl. Phys. **B250**, 199 (1985).

[52] F. Landry, R. Brock, P. M. Nadolsky, and C. P. Yuan, Phys. Rev. D **67**, 073016 (2003).

[53] J. Beringer *et al.* (Particle Data Group), Phys. Rev. D **86**, 010001 (2012).

[54] S. Frixione, P. Nason, and C. Oleari, J. High Energy Phys. 11 (2007) 070.

[55] S. Alioli, P. Nason, C. Oleari, and E. Re, J. High Energy Phys. 07 (2008) 060.

[56] G. A. Ladinsky and C. P. Yuan, Phys. Rev. D **50**, R4239 (1994).

[57] C. Balazs and C. P. Yuan, Phys. Rev. D **56**, 5558 (1997).

[58] T. Becher, C. Lorentzen, and M. D. Schwartz, Phys. Rev. Lett. **108**, 012001 (2012).

[59] J. Rojo (private communication).